SRS 16-86 attenuation of ferroptosis and promotion of recovery in diabetic nephropathy

Yingchun Qiao[1], Chao Sun[2], Shunli Kan[3], Lu He[1], Yawen Wang[1], Huajun Gao[1], Yingying Zhang[1], You Cheng[1], Shuai Wang[1], Long Zhao[2], and Wenyan Niu[1]

[1]Chu Hsien-I Memorial Hospital & Tianjin Institute of Endocrinology Tianjin Medical University - NHC Key Laboratory of Hormones and Development, Tianjin Key Laboratory of Metabolic Diseases
[2]International Science and Technology Cooperation Base of Spinal Cord Injury Tianjin Key Laboratory of Spine and Spinal Cord Injury
[3]Tianjin Union Medical Center

January 30, 2024

Abstract

Diabetic nephropathy (DN) is a common complication of diabetes mellitus and cell death is a key issue in DN. Ferroptosis is a recently discovered type of iron-dependent cell death and different from other kinds of cell death including apoptosis and necrosis. However, ferroptosis has not been described in the context of DN. This study was to explore the role of ferroptosis in the DN pathophysiology and to explore the efficacy of ferroptosis inhibitor SRS 16-86 on DN. The STZ injection was used to establish the DM and DN animal models. We detected the levels of iron, reactive oxygen species, and ferroptosis-specific markers in a rat DN model to investigate whether there was ferroptosis in the process of DN. The hematoxylin-eosin staining, blood biochemistry, urine biochemistry and the of function kidney were used to evaluate the efficacy of ferroptosis inhibitor-SRS 16-86 in repairing DN. We found that SRS 16-86 could improve the recovery of renal function after DN by improving the antiferroptosis factors glutathione peroxidase 4, glutathione, and system Xc-light chain and could lower the lipid peroxidation marker and 4-hydroxynonenal. SRS 16-86 treatment may improve the structure of renal organization after DN. Inflammatory cytokines-interleukin 1β and tumor necrosis factor α, and intercellular adhesion molecule 1 were decreased significantly following SRS 16-86 treatment after DN. Results indicate that there is a strong connection between ferroptosis and the pathological mechanism of DN. The validity of SRS 16-86, a ferroptosis inhibitor in DN repair, supports its potential as a new therapeutic target for DN.

Original Article

SRS 16-86 attenuation of ferroptosis and promotion of recovery in diabetic nephropathy

Yingchun Qiao[1#], Chao Sun[2#], Shunli Kan[3#], Lu He[1], Yawen Wang[1], Huajun Gao[1], Yingying Zhang[1], You Cheng[1], Shuai Wang[1], Long Zhao[2], Wenyan Niu[1]

[1]NHC Key Laboratory of Hormones and Development, Tianjin Key Laboratory of Metabolic Diseases, Department of Clinical Laboratory, Chu Hsien-I Memorial Hospital & Tianjin Institute of Endocrinology, Tianjin Medical University, Tianjin, China;[2]International Science and Technology Cooperation Base of Spinal Cord Injury, Tianjin Key Laboratory of Spine and Spinal Cord Injury, Department of Orthopedics, Tianjin Medical University General Hospital, Tianjin Medical University, Tianjin, China; [3]Department of Spine Surgery, Tianjin Union Medical Center, Tianjin, China

#These authors contributed equally to this work.

Correspondence to: Wenyan Niu. NHC Key Laboratory of Hormones and Development, Tianjin Key Laboratory of Metabolic Diseases, Department of Clinical Laboratory, Chu Hsien-I Memorial Hospital & Tianjin Institute of Endocrinology, Tianjin Medical University, Tianjin, China. Email:*wniu@tmu.edu.cn* .

#Abstract

Diabetic nephropathy (DN) is a common complication of diabetes mellitus and cell death is a key issue in DN. Ferroptosis is a recently discovered type of iron-dependent cell death and different from other kinds of cell death including apoptosis and necrosis. However, ferroptosis has not been described in the context of DN. This study was to explore the role of ferroptosis in the DN pathophysiology and to explore the efficacy of ferroptosis inhibitor SRS 16-86 on DN. The STZ injection was used to establish the DM and DN animal models. We detected the levels of iron, reactive oxygen species, and ferroptosis-specific markers in a rat DN model to investigate whether there was ferroptosis in the process of DN. The hematoxylin-eosin staining, blood biochemistry, urine biochemistry and the of function kidney were used to evaluate the efficacy of ferroptosis inhibitor-SRS 16-86 in repairing DN. We found that SRS 16-86 could improve the recovery of renal function after DN by improving the antiferroptosis factors glutathione peroxidase 4, glutathione, and system Xc-light chain and could lower the lipid peroxidation marker and 4-hydroxynonenal. SRS 16-86 treatment may improve the structure of renal organization after DN. Inflammatory cytokines-interleukin 1β and tumor necrosis factor α, and intercellular adhesion molecule 1 were decreased significantly following SRS 16-86 treatment after DN. Results indicate that there is a strong connection between ferroptosis and the pathological mechanism of DN. The validity of SRS 16-86, a ferroptosis inhibitor in DN repair, supports its potential as a new therapeutic target for DN.

Keywords : Ferroptosis; diabetic nephropathy; ferroptosis inhibitor

 # Introduction

Diabetic nephropathy (DN) is a common complication of type 1 and type 2 diabetes mellitus (DM)(1). DN affects approximately 40% of people with DM and is the leading cause of chronic kidney disease and end-stage renal disease worldwide(2). Glomerular destruction leads to kidney damage, proteinuria, and hypertension(3). Apoptosis, autophagy, and necrosis are three forms of programmed cell death and are involved in the pathogenesis of DN. Podocyte apoptosis leads to glomerular injury and podocyte failure, which is related to proteinuria and glomerular structural damage in DN(4). In the DN process, the epithelial cells of the proximal convoluted tubules also undergo apoptosis, leading to tubular atrophy, the reduction of tubular cells, and the formation of glomeruli, which ultimately contributes to the loss of renal function(5). On the other hand, the dysfunction of autophagy may also cause the pathogenesis of DN. More specifically, the decrease of podocyte autophagy activity in diabetes kidneys leads to changes in podocyte function, which then destroys the glomerular filtration barrier(6). In addition, the autophagic activity of renal proximal tubular cells in diabetes is weakened, leading to the accumulation of damaged molecules and organelles, which are usually decomposed by autophagy, and this causes proteinuria(7). In addition, necrosis may play a key role in podocyte injury and the subsequent worsening of DN(8). Indeed, the pattern of cell death in DN has been intensely researched. Apoptosis and necrosis are among of the causes of acute DN cell injury, and autophagy seems to have beneficial effects on DN. However, ferroptosis has not been described in the context of DN.

In 2012, Dixon et al. studied the mechanism of erastin killing cancer cells through renin-angiotensin system (*RAS*) mutation and formally named this cell death process *ferroptosis* (9). In the process of ferroptosis, there is no morphological change in cell membrane or chromatin, which primarily suggests that the volume and cristae of mitochondria decreases while the density of the mitochondrial membrane increases(10). Biochemically, the main manifestations of ferroptosis are the decrease of glutathione peroxidase 4 (GPX4) activity, the loss of intracellular glutathione, and the increase of reactive oxygen species (ROS) level(11). The

accumulation of iron and the consumption of glutathione and lipid peroxidation are indispensable and occur simultaneously in the process of ferroptosis(12). Inhibiting lipid peroxidation can prevent the cell death stage of ferroptosis. Ferroptosis is associated with inflammatory processes in which cell-released substances are significantly involved in the innate immune system and control cellular inflammatory responses, signal transduction, and cell proliferation. Ruptured ferroptosis associated cells release damage-related molecular patterns. And ferroptosis leads to the infiltration of macrophages and neutrophils and the release of inflammatory cytokines. When the accumulation of lipid ROS exceeds a certain threshold, a large number of pro-inflammatory cytokines are produced, such as interleukin 1β (IL-1β) and tumor necrosis factor α (TNF-α). Iron overload and lipid ROS have been shown, in vitro, to be the two main factors causing ferroptosis in tumor cells and brain slices, which have been reported in DN. DN leads to ROS accumulation, and bleeding increases the iron load in this process(13). Glutamic acid could also induce the death of podocyte cells. After DN, the level of glutamic acid increases, and glutamate excitotoxicity becomes apparent. GPX4 expression decreased and lipid peroxidation products increased in the animal model of DN and the DN patients' blood. Therefore, we speculated that ferroptosis in DN contributes to its damage. And the inhibition of ferroptosis could reduce functional damage and improve renal repair.

It is a question worthy of investigation that whether specific inhibitors of ferroptosis could promote renal repair, and in vivo research to identify effective and stable specific inhibitor of ferroptosis is warranted. Ferrostatin 1 (Fer-1) is a first-generation ferroptosis inhibitor, possessing demonstrated ability to inhibit ferroptosis in vitro. However, due to the instability of plasma and metabolism, its internal function is weak. SRS 16-86 is a third-generation small-molecule which could restrain lipid ROS. It has been reported to strongly inhibit ferroptosis in renal failure with ischemia reperfusion injury.

We hypothesized that ferroptosis is an important damage mechanism after DN. Specifically, we studied whether ferroptosis occurs in DN and SRS 16-86 to inhibit ferroptosis could improve the recovery of renal function. The insights earned from our study could promote the understanding of the process in DN and support new therapeutic method for treating DN.

#Methods

##Animals

The 6 weeks-age of male Sprague-Dawley rats weighing 160–180 g were purchased from the Laboratory Animal Center of the Academy of Military Medical Sciences (Beijing, China). The animals were placed in a humidity- and temperature-controlled environment, with a light cycle of 12 h, with 3 animals in each cage, and free access to food and water. Experiments were performed under a project license (No. IRM-DWLL-2020019) granted by Ethics Committee of the Institute of Radiation Medicine, Chinese Academy of Medical Science & Peking Union Medical College, in compliance with institutional guidelines for the care and use of animals. A protocol was prepared and passed our team's proposal report before the study, while with no registration as it's not a clinical trial.

##Experimental groups

Sprague-Dawley rats were intraperitoneally injected with 40 mg/kg of newly prepared streptozotocin once to cause diabetes, and normal control animals were intraperitoneally injected with the same amount of citric acid buffer. The dose of SRS 16-86 was 15 mg/kg as this does of SRS 16-86 was safe and effective for repairing spinal cord injury animal model. We selected 6 animals from each group at each time point to ensure the accuracy of the data. Animals (n=150) were randomly assigned to the following groups without exclusions and only the designer of experiment (Yingchun Qiao) was aware of the group allocation at the different stages of the experiment: control group, Sprague-Dawley rats + citrate buffer (n=50); DN group, Sprague-Dawley rats + streptozotocin (STZ) (n=50); and DN-SRS group, SD rats + STZ + SRS 16-86 (n=50).

All aspects of testing and data analysis employed a blinded design.

##Iron assay

Renal tissue samples (10 mg) from each group were washed with cold normal saline after incision. A vibrating homogenizer was immediately applied to add cold brine for tissue homogenization. In addition, the collected cells were homogenized with ultrasonic cell interfering agent. After centrifugation for 10 min, the supernatant was collected, and the iron concentration in tissues and cells was determined with an iron content determination kit (BioAssay, Hayward, CA, USA). According to the manufacturer's instructions, a sufficient amount of the working reagents was prepared, the working reagents were transferred with 96-well plate, and supernatant was collected from a 96-well plate. The optical density determination wavelength of the iron content determination kit was 590 nm.

##Western blot

Kidneys were collected and placed in a solution (300) containing with 20 mM of Tris pH 7.4, 50 mM of NaCl, 1% Triton X-100, and protease inhibitor 10 μL for homogeneous cracking in cracking liquid. Protein samples were taken out at –80 and refrigerated to reduce protein degradation. The sample was placed in sodium dodecyl sulfate gel loaded buffer solution, boiled for 5 min and centrifuged at 4 at 6,000 rpm for 3 min, after which the supernatant was collected. The denatured protein underwent electrophoresis in gel and was then transferred to the polyvinylidene fluoride membrane for 2 hours at 65 V and 4 through a transfer device. After blocking on a shaking table at room temperature was conducted for 2 hours, the first antibody was incubated at 4 overnight. This was followed by 3 washes with Tris-buffered saline with Tween. After 10 minutes washing, goat anti-rabbit immunoglobin G combined with horseradish peroxidase (1:2000; Sigma-Aldrich) was added and incubated for 1.5 h. The membrane was washed with TBST and observed with an enhanced chemiluminescence system.

##ROS and glutathione detection

The kidney homogenate was prepared at a low temperature. An ROS test kit (Beyotime) and a total glutathione test kit (Beyotime) were used to test the reactive oxygen species (ROS) level and glutathione (GSH) level, respectively, according to the manufacturer's instructions.

##Hematoxylin and eosin stanning

Hematoxylin and eosin (HE) staining was used to evaluate the histological structure of each group. After anesthesia, the rats were perfused with 0.9% NaCl and 4% paraformaldehyde through their cranium. Kidney tissue was extracted and soaked in 4% paraformaldehyde at 4 for one day. Following this, paraffin-embedded, 5-μm thick sections were stained with HE.

##Statistical analysis

Statistical analysis was conducted through GraphPad Prism 9.0 software (GraphPad Software, San Diego, CA, USA). The student t test was used for pairwise comparisons. Single factor analysis of variance was used for comparison among multiple groups, and Bonferroni correction was performed. Data are expressed as mean ± standard error of the mean (SEM). The difference was considered statistically significant at a P value <0.05.

#Results

##Establishment of DM and DN animal models

We induced diabetes models according to the protocols of Animal Models of Diabetic Complications Consortium. Sprague-Dawley rats weighing 160–180 g were induced to diabetes with a single 60 mg/kg intraperitoneal injection of freshly prepared STZ (Figure 1A). The DN-SRS group was then treated with intraperitoneal injection of SRS 16-86 at a dose of 15 mg/kg once/day from week 1 to week 8 after STZ treatment, while the DN group was treated with the same dose of dimethylsulfoxide (DMSO) (Figure 1A). Blood glucose in the DN and DN-SRS groups was significantly higher than that in the control group 3 days after STZ treatment; moreover, both the DN and DN-SRS groups' body weight was significantly lower than that in the control group, proving that the diabetic animal model was successfully constructed (Figure 1B,1C). We evaluated renal function changes by measuring 24-hour urine volume, creatinine (CRE2U), and urine total

protein (UTP). As shown in Figure 2, 24-hour urine volume and the content of CRE2U and UTP in the DN and DN-SRS groups were markedly higher than those of control group at the 8-week time point, indicating that the DN animal model was successfully constructed (Figure 2A,2B,2C).

##Reduced overload of iron by ferroptosis inhibition

Iron overload plays an important role in oxidative stress, and the accumulation and lipid peroxidation of Fe^{2+} are the key factors of ferroptosis. To explore SRS 16-86 on overload of iron on DN, an iron ion detection kit was used to measure the iron content. In this study, the overload of iron in the DM group was significantly increased compared with that in the control group, while SRS 16-86 treatment could reduce the content of iron compared with the DN group, indicating a reduced overload of iron (Figure 3A).

##SRS 16-86 downregulated the expression of ROS and 4-hydroxynonenal level in DN

Ferroptosis is caused by the lipid peroxidation induced by ROS accumulation: ROS decomposition produces malondialdehyde (MDA) and 4-hydroxynonenal (4-HNE), which then form covalent adjuncts with proteins, DNA, lipids, and other macromolecules to cross-link and inactivate proteins that promote ferroptosis, thus precipitating cell membrane rupture and ferroptosis. In this study, we detected the ROS (Figure 3B) and 4HNE (Figure 4A,4D) expressions. 4HNE and ROS levels were significantly upregulated post-DN in the DN group compared to the control group. After treatment with SRS 16-86, 4HNE and ROS expression was upregulated, demonstrating that SRS 16-86 could inhibit lipid peroxidation.

##SRS 16-86 upregulated thelevel of xCT, GSH, and GPX4 in DN

The xCT-GSH-GPX4 axis contributed to the negative regulation of ferroptoptic-related cell death. High extracellular glutamate levels can inhibit systemic xCT activity and thus induce ferroptosis. We detected the expression of xCT, GPX4, and GSH post-DN (Figure 4A,4B,4C,4E). xCT, GPX4, and GSH levels were significantly reduced post-DN in the DN group compared to the control group. These results indicated that the capacity of peroxidation repair in the kidneys of diabetic rats was dramatically reduced. We also found that the expression of xCT, GPX4, and GSH were upregulated after treatment with SRS 16-86. The antioxidant capacity was repaired in the SRS group.

##Reduction of DN inflammation by ferroptosis inhibitor

Ferroptosis is involved in mediating the inflammatory response. The expression of interleukin (IL)-1β, tumor necrosis factor (TNF)-α, and intercellular adhesion molecule 1 (ICAM-1) were assessed by Western blotting post-DN to clarify the content of inflammation (Figure 5A,5B,5C,5D). The IL-1β, TNF-α, and ICAM-1 in the kidneys of rats in the DN group was significantly increased compared to the control group. SRS 16-86 attenuated the levels of expression. SRS 16-86 decreased the levels of inflammatory cytokines in the kidneys of rats with DN.

##Improvement of theorganizational structure after DN via the inhibition of ferroptosis

To explore whether SRS 16-86 modulates the organizational structure after DN, we examined the kidneys of rats in each group with HE staining (Figure 6). In comparison to kidneys in the control group, obvious disorder was visible on the section of the kidneys in the DN group. In the DN group, the glomerular morphology was abnormal, the renal tubule space was enlarged, and renal tissue fibrosis was enhanced. Meanwhile, the DN-SRS group showed an improvement of organizational structure when compared with the DN group. These results show that SRS 16-86 significantly reduced destruction of the organizational structure as evidenced by the increased amount of spared normal tissue and the decreased extent of lesions, which were associated with improved renal function recovery.

##Improved renal function recovery after DN via the inhibition of ferroptosis

To explore whether SRS 16-86 could improve renal function recovery after DN, we examined the expression of 24-hour urine volume and CRE2U and UTP content in urine and uric acid (UA) as well as the UREA and creatinine (CRE) content in blood (Figure 7A,7B,7C; Figure 8A,8B,8C). As was shown in Figure 2, 24-hour

urine volume and the content of CRE2U and UTP in the DN-SRS group were remarkably lower than those in the DN group. We observed the same pattern of change in assessments of UA, UREA and CRE. These results showed SRS 16-86 significantly promoted renal function recovery after DN.

#Discussion

Ferroptosis is a newly discovered cell death pathway, which has been confirmed in stroke, Parkinson disease, and spinal cord injury(14-15). However, ferroptosis in DN has not been reported on. We found that the key regulatory factors of ferroptosis, including GPX4, GSH, and xCT were reduced in DN. Meanwhile, tests for ROS and 4HNE indicated that lipid peroxidation level was added. By analyzing tissue structure and renal function after SRS 16-86 inhibited ferroptosis, we found that inhibiting ferroptosis could increase the survival of normal tissue structure and improve the recovery of renal function. Inflammatory cytokines also decreased after SRS 16-86 treatment. Experimental evidence supporting the beneficial effect of ferroptosis interference opens new avenues of treatment for reducing cell death and promoting DN repair.

Excess iron in tissue cells induces cell death by producing ROS through the Fenton reaction. Additionally, GPX4 inactivation due to GSH depletion can also lead to ROS accumulation through lipid peroxidation(16-17). ROS can react with polyunsaturated fatty acids (PUFAs) in lipid membranes and induce lipid peroxidation. A study has shown that ferroptosis is closely regulated by the combination of several signaling pathways, including the regulation of iron homeostasis, the RAS/rapidly accelerated fibrosarcoma (RAF) signaling pathway and the glutamine-cystine transport signaling pathway(18-19). Factors such as GSH and GPX4 play key roles in the ferroptoptic process. GSH removes excessive ROS from the body through GPX4, thus protecting the body from damage. Once the dynamic GSH-GPX4-ROS balance is destroyed, the excessive ROS generated by the body cannot be removed in time, which causes certain damage to the body. GPX4 deficiency has been found to lead to significantly elevated iron death in the epithelial cells of the renal tubules, resulting in acute renal failure(20). It has been found that the increase of glutamate can promote the activation of glutamate-glutathione transporter, allowing glutamate to enter the cell to produce excessive ROS and induce ferroptosis(21). SRS 16-86 is a newly more stable and effective synthesized iron-droop inhibitor(22-23). It has a strong protective effect on renal ischemia-reperfusion injury. In our DN model, SRS 16-86 increased the concentration of GSH in renal tissue and decreased the lipid ROS marker 4HNE. GPX4 and xCT are markers of ferroptosis. The expression of GPX4 and xCT was downregulated after injury and increased after inhibition treatment. These results indicate that SRS 16-86 inhibiting the ferroptosis process. HE staining showed that more tissues were retained after inhibitor treatment.

Inflammation is an immune response that is produced by the body according to changes in the internal and external environment of cells. Moderate immune reaction can protect the body, while excessive immune reaction can cause harm to the body. The process of ferroptosis is often accompanied by inflammation(24-26). In a mouse model of folic acid induced acute renal injury, necrosis and inflammation accompanied by ferroptosis led to the death of a large number of renal tubular cells, causing acute renal failure and early death(27). In our study, SRS 16-86 treatment reduced the expression of proinflammatory cytokine IL-1 β, TNF-α, and ICAM-1 which suggesting that inhibition of ferroptosis may also lead to the blocking of the inflammatory cascade in DN. Lipid peroxidation in ferroptosis can produce inflammatory signal molecules. This was consistent with the effect of Fer-1 on reducing proinflammatory cytokines in the acute renal injury model. However, whether ferroptosis is related to the inflammatory microenvironment of DN is a question that remains to be further studied.

Indications that the ferroptosis pathway is related to the secondary injury of DN has opened up exploration of this problem. (I) GSH exhaustion and lipid peroxidation have been observed in DN, but GPX4 and other essential factors for iron removal in DN is still unclear. The exploring of these factors could provide new ways into the pathophysiology of DN. (II) Moreover, the sensitivity of the different types of cells in DN to ferroptosis is unclear. In our study, we found that in the DN group, the glomerular morphology was abnormal, the gap between renal tubules was enlarged, and renal fibrosis was enhanced. However, the extent to which cells in each tissue are affected remains unknown. It's important to determine whether other known drugs could promote DN by inhibiting ferroptosis. Studying ferroptosis may elucidate the mechanism

of traditional medicine and provide a new direction for treatment.

#Conclusions

In conclusion, we demonstrated that ferroptosis playing an important role in pathophysiological process of DN by using SRS 16-86 to treat DN. This inhibitor may be an effective method for treating patients with DN.

Conflicts of Interest

The authors have no conflicts of interest to declare.

Acknowledgments

Funding: The study was supported by Scientific Research Funding of Tianjin Medical University Chu Hsien-I Memorial Hospital (No. 2018ZDKF10, 2019ZDKF02 and 2019ZDKF08), Funding of Tianjin Educational Committee (No.2022KJ242) and Funding of Tianjin Health Research Project (No. ZC20225 and KJ20061).

References

1. Li X, Lu L, Hou W, et al. Epigenetics in the pathogenesis of diabetic nephropathy. Acta Biochim Biophys Sin (Shanghai) 2022;54:163-72.
2. Tu X, Luo N, Lv Y, et al. Prognostic evaluation model of diabetic nephropathy patients. Ann Palliat Med 2021;10(6):6867-6872.
3. Samsu N. Diabetic Nephropathy: Challenges in Pathogenesis, Diagnosis, and Treatment. Biomed Res Int 2021;2021:1497449.
4. Barutta F, Bellini S, Gruden G. Mechanisms of podocyte injury and implications for diabetic nephropathy. Clin Sci (Lond) 2022;136:493-520.
5. Ma X, Hao C, Yu M, et al. Investigating the Molecular Mechanism of Quercetin Protecting against Podocyte Injury to Attenuate Diabetic Nephropathy through Network Pharmacology, MicroarrayData Analysis, and Molecular Docking. Evid Based Complement Alternat Med 2022;2022:7291434.
6. Erekat NS. Programmed Cell Death in Diabetic Nephropathy: A Review of Apoptosis, Autophagy, and Necroptosis. Med Sci Monit 2022;28:e937766.
7. Barutta F, Bellini S, Kimura S, et al. Protective effect of the tunneling nanotube-TNFAIP2/M-sec system on podocyte autophagy in diabetic nephropathy. Autophagy 2022. [Epub ahead of print]. doi: 10.1080/15548627.2022.2080382.
8. Morimoto K, Matsui M, Samejima K, et al. Renal arteriolar hyalinosis, not intimal thickening in large arteries, is associated with cardiovascular events in people with biopsy-proven diabetic nephropathy. Diabet Med 2020;37:2143-52.
9. Dixon SJ, Lemberg KM, Lamprecht MR, et al. Ferroptosis: an iron-dependent form of nonapoptotic cell death. Cell 2012;149:1060-72.
10. Basit F, van Oppen LM, Schöckel L, et al. Mitochondrial complex I inhibition triggers a mitophagy-dependent ROS increase leading to necroptosis and ferroptosis in melanoma cells. Cell Death Dis 2017;8:e2716.
11. Zheng D, Liu J, Piao H, et al. ROS-triggered endothelial cell death mechanisms: Focus on pyroptosis, parthanatos, and ferroptosis. Front Immunol 2022;13:1039241.
12. Perez MA, Clostio AJ, Houston IR, et al. Ether lipid deficiency disrupts lipid homeostasis leading to ferroptosis sensitivity. PLoS Genet 2022;18:e1010436.
13. Qiao L, Liu Y, Li C, et al. Regulation of iRhom-2/Tumor Necrosis Factor-α Converting Enzyme Pathway and Oxidative Stress Protects the Renal Injury with Anemonin in Streptozotocin-Induced Diabetic Nephropathy Neonatal Rat Model. Pharmacology 2019;104:258-66.
14. Zhang Y, Sun C, Zhao C, et al. Ferroptosis inhibitor SRS 16-86 attenuates ferroptosis and promotes functional recovery in contusion spinal cord injury. Brain Res 2019;1706:48-57.
15. Ashraf A, Jeandriens J, Parkes HG, et al. Iron dyshomeostasis, lipid peroxidation and perturbed

expression of cystine/glutamate antiporter in Alzheimer's disease: Evidence of ferroptosis. Redox Biol 2020;32:101494.
16. Sugezawa K, Morimoto M, Yamamoto M, et al. GPX4 Regulates Tumor Cell Proliferation via Suppressing Ferroptosis and Exhibits Prognostic Significance in Gastric Cancer. Anticancer Res 2022;42:5719-29.
17. Zhang J, Xie H, Yao J, et al. TRIM59 promotes steatosis and ferroptosis in non-alcoholic fatty liver disease via enhancing GPX4 ubiquitination. Hum Cell 2023;36:209-22.
18. Ma T, Du J, Zhang Y, et al. GPX4-independent ferroptosis-a new strategy in disease's therapy. Cell Death Discov 2022;8:434.
19. Xu W, Sun T, Wang J, et al. GPX4 Alleviates Diabetes Mellitus-Induced Erectile Dysfunction by Inhibiting Ferroptosis. Antioxidants (Basel) 2022;11:1896.
20. Dixon SJ, Patel DN, Welsch M, et al. Pharmacological inhibition of cystine-glutamate exchange induces endoplasmic reticulum stress and ferroptosis. Elife 2014;3:e02523.
21. Xie Z, Xu M, Xie J, et al. Inhibition of Ferroptosis Attenuates Glutamate Excitotoxicity and Nuclear Autophagy in a CLP Septic Mouse Model. Shock 2022;57:694-702.
22. Fan BY, Pang YL, Li WX, et al. Liproxstatin-1 is an effective inhibitor of oligodendrocyte ferroptosis induced by inhibition of glutathione peroxidase 4. Neural Regen Res 2021;16:561-6.
23. Shi Q, Liu R, Chen L. Ferroptosis inhibitor ferrostatin-1 alleviates homocysteine-induced ovarian granulosa cell injury by regulating TET activity and DNA methylation. Mol Med Rep 2022;25:130.
24. Astudillo AM, Balboa MA, Balsinde J. Compartmentalized regulation of lipid signaling in oxidative stress and inflammation: Plasmalogens, oxidized lipids and ferroptosis as new paradigms of bioactive lipid research. Prog Lipid Res 2022. [Epub ahead of print]. doi: 10.1016/j.plipres.2022.101207.
25. Zhao Y, Zhao Y, Tian Y, et al. Metformin suppresses foam cell formation, inflammation and ferroptosis via the AMPK/ERK signaling pathway in ox-LDL-induced THP-1 monocytes. Exp Ther Med 2022;24:636.
26. Zhu G, Sui S, Shi F, et al. Inhibition of USP14 suppresses ferroptosis and inflammation in LPS-induced goat mammary epithelial cells through ubiquitylating the IL-6 protein. Hereditas 2022;159:21.
27. Tao WH, Shan XS, Zhang JX, et al. Dexmedetomidine Attenuates Ferroptosis-Mediated Renal Ischemia/Reperfusion Injury and Inflammation by Inhibiting ACSL4 via α2-AR. Front Pharmacol 2022;13:782466.

Figures and figure Legends

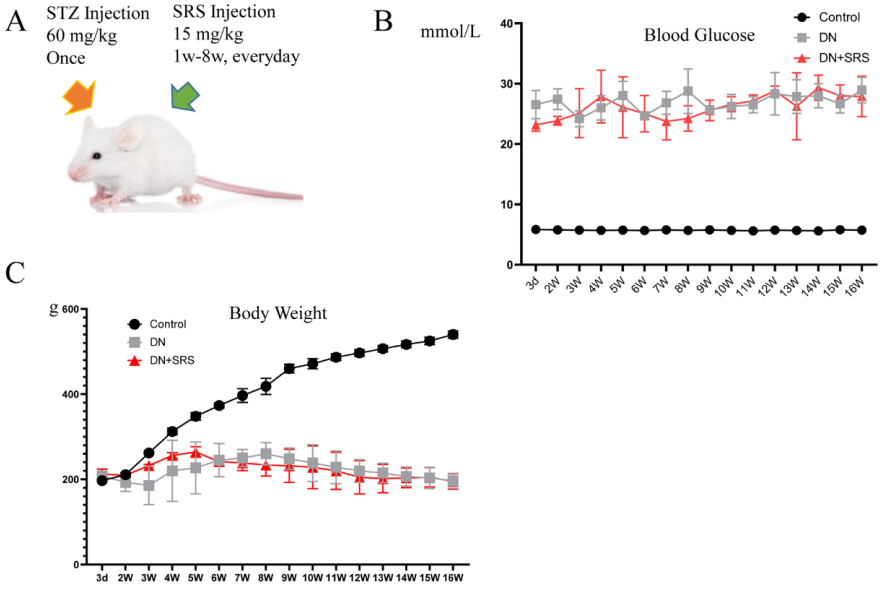

Figure 1. Establishment of the diabetes mellitus and diabetic nephropathy (DN) animal models. (A) A diabetes mellitus (DM) animal model was established with a single intraperitoneal injection of freshly prepared streptozotocin (60 mg/kg); the DN-SRS group was treated with am intraperitoneal injection of SRS 16-86 with the dose of 15 mg/kg once/day from week 1 to 8 week after STZ treatment. (B, C) Blood glucose and body weight after STZ treatment (n=6).

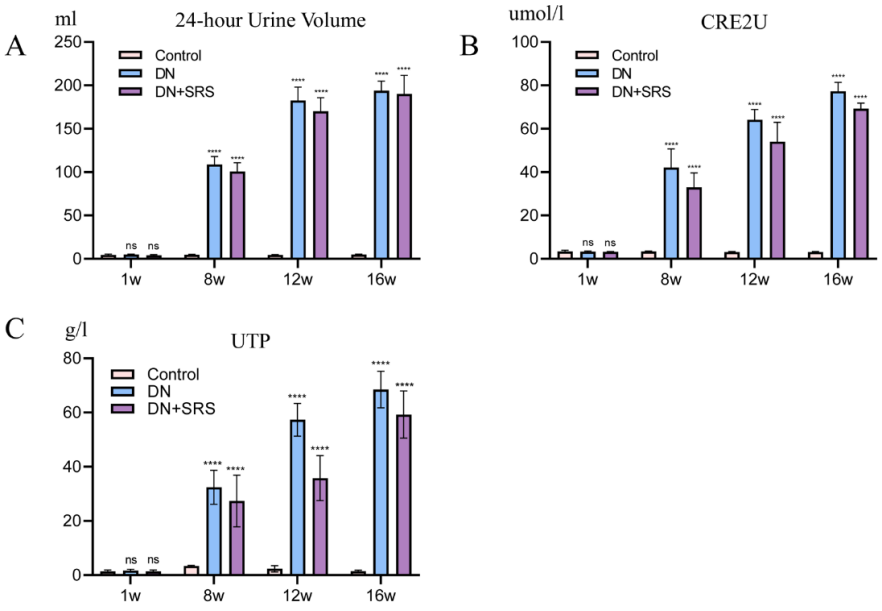

Figure 2. 24-hour urine volume, creatinine (CRE2U), and urine total protein (UTP) after streptozotocin treatment. 24-hour urine volume and the content of CRE2U and UTP in the DN and DN-SRS groups were markedly higher than those control group at the 8-week time point after STZ treatment, proving that the diabetic nephropathy animal model was successfully constructed (n=6/group). (ns:P>0.05; *P<0.05; **P<0.01; ***P<0.001; ****P<0.0001)

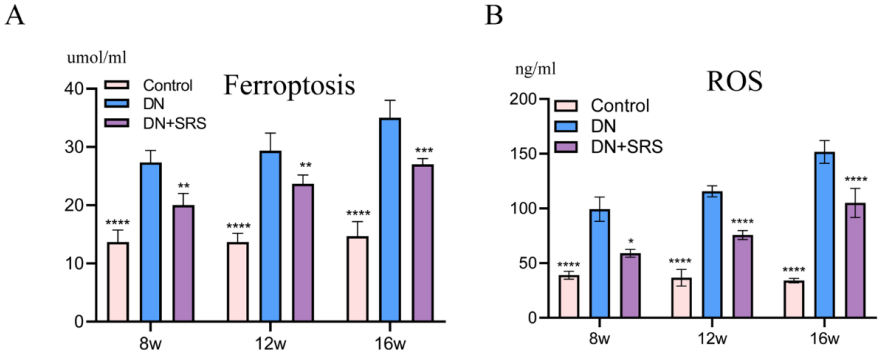

Figure 3 Reduced overload of iron and reactive oxygen species (ROS) expression via the inhibition of ferroptosis. The overload of iron and ROS expression in the DM group were significantly increased compared with the control group, while SRS 16-86 treatment could reduce the content of iron compared with the DN group (n=6/group). (ns:P>0.05; *P<0.05; **P<0.01; ***P<0.001; ****P<0.0001)

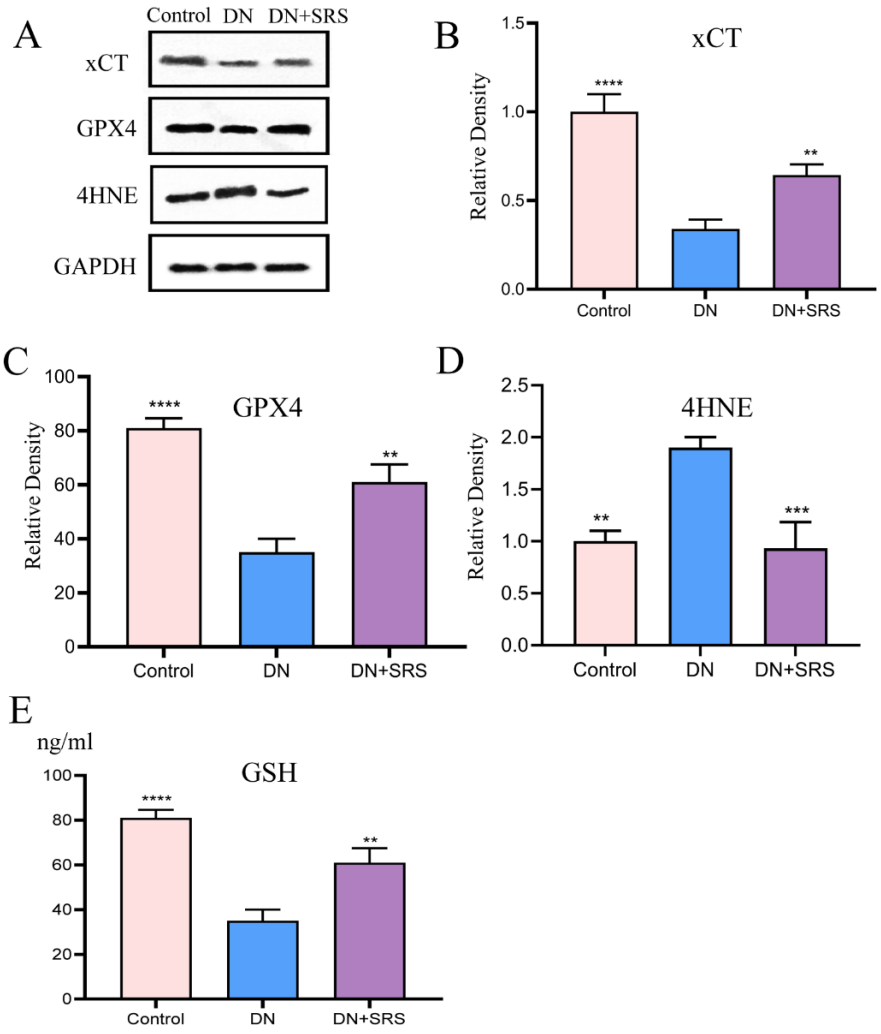

Figure 4. SRS 16-86 u-regulated system Xc-light chain (xCT), glutathione (GSH), and glutathione peroxidase 4 (GPX4) level and downregulated 4-hydroxynonenal (4HNE) level in diabetic nephropathy rats. The expression of xCT, GPX4, and GSH were increased while that of 4HNE was decreased after treatment with SRS 16-86 (n=6/group). (ns:P>0.05; *P<0.05; **P<0.01; ***P<0.001; ****P<0.0001)

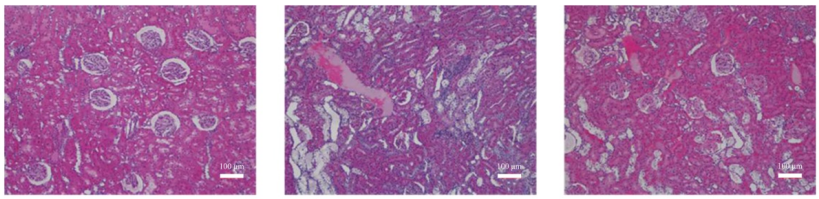

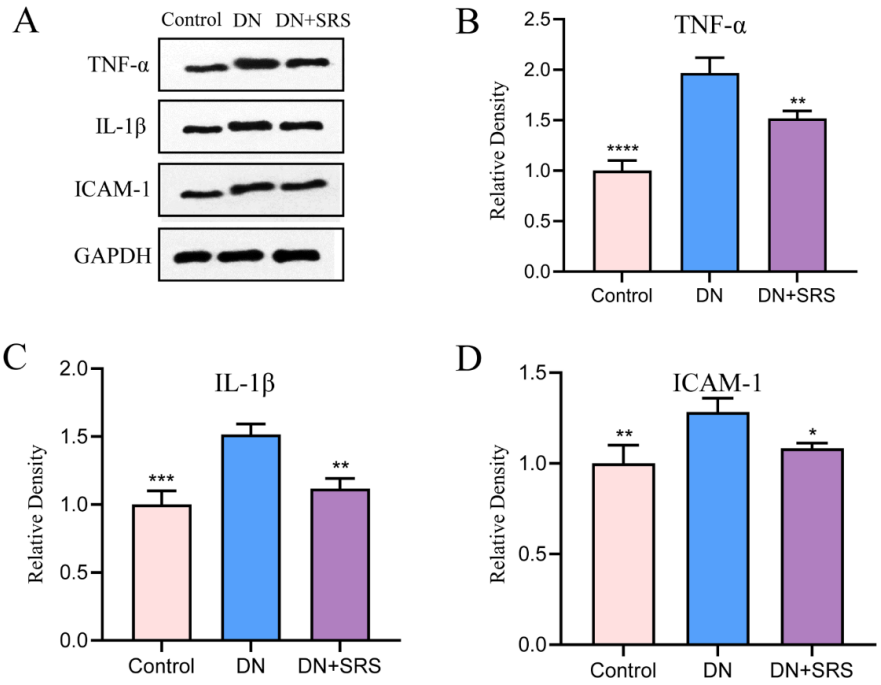

Figure 5. Reduction of DN inflammation by ferroptosis inhibitor. Expression of tumor necrosis factor α (TNF-α), interleukin 1β (IL-1β) and intercellular adhesion molecule 1 (ICAM-1) in the kidneys of rats in the DN group significantly increased in comparison to the control group. Treatment with the SRS 16-86 attenuated the levels of expression (n=6/group). (ns:P>0.05; *P<0.05; **P<0.01; ***P<0.001; ****P<0.0001)

Figure 6. Improvement of organizational structure after DN via the inhibition of ferroptosis. Obvious disorder was visible on the transverse section of the kidney with the HE staining after DN while SRS 16-86 treatment significantly reduced destruction of the organizational structure (n=6/group).

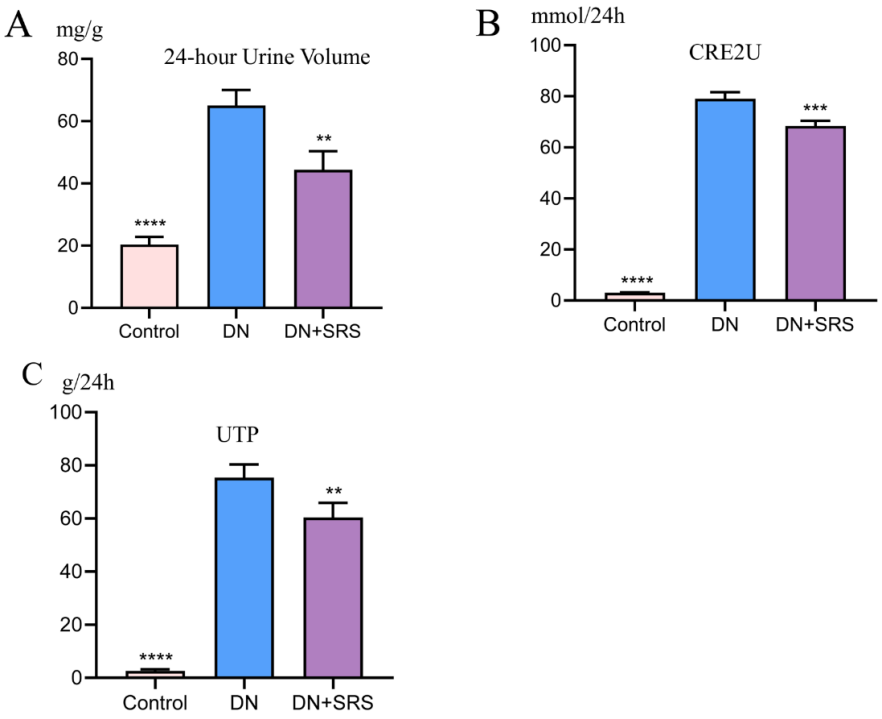

Figure 7. Improved renal function recovery after DN via the inhibition of ferroptosis. 24-hour urine volume and the content of CRE2U and UTP in the DN-SRS group were markedly lower than those in the DN group (n=6/group). (ns:P>0.05; *P<0.05; **P<0.01; ***P<0.001; ****P<0.0001)

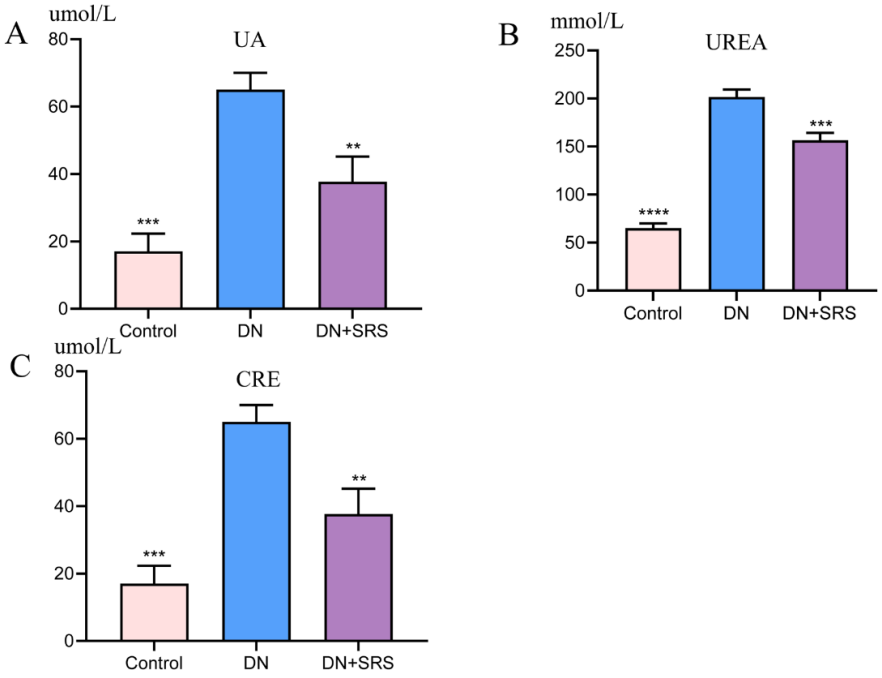

Figure 8. Improved renal function recovery after DN via the inhibition of ferroptosis. The content of uric

acid (UA), UREA and creatinine (CRE) in the DN-SRS group was markedly lower than that in the DN group (n=6/group). (ns:P>0.05; *P<0.05; **P<0.01; ***P<0.001; ****P<0.0001)